JOURNAL OF CATALYSIS 67, 186–206 (1981)

Determination of Metal Crystallite Size and Morphology in Supported Nickel Catalysts

DONALD G. MUSTARD AND CALVIN H. BARTHOLOMEW

Catalysis Laboratory, Department of Chemical Engineering, Brigham Young University, Provo, Utah 84602

Received May 8, 1980; revised July 7, 1980

The application of H_2 chemisorption, X-ray diffraction (XRD) line broadening, and transmission electron microscopy (TEM) to the determination of metal crystallite size and size distribution in Ni/SiO_2, Ni/Al_2O_3, and Ni/TiO_2 catalysts having wide ranges of nickel loadings and dispersions was investigated. Average crystallite diameters estimated from H_2 chemisorption and TEM were found to be in very good agreement over wide ranges of metal dispersion and loading in the Ni/SiO_2 system and in good agreement for a 15% Ni/Al_2O_3; poor agreement was evident in the Ni/TiO_2 system, the results suggesting that H_2 adsorption was suppressed. In the few samples where it was possible to obtain information from XRD, the estimates of crystallite diameter were generally in good or fair agreement with those from H_2 chemisorption or TEM. The specific limitations of these three techniques in determination of nickel crystallite size and their application to the study of sintering and metal support interactions in supported nickel catalysts are presented and discussed.

INTRODUCTION

Nickel catalysts find application in a number of important industrial processes, for example, hydrogenation of unsaturated organics, steam reforming, and methanation. Therefore, determination of their physical properties is of considerable practical value. Nickel metal particle size is one of the most important properties, since it is a measure of metal dispersion, i.e., the number of surface sites available in the catalyst for promoting the reaction. Since in industrial applications, metal particle size and metal surface area change with time because of catalyst degradation (i.e., sintering, poisoning, and coking), the measurement of these properties as a function of time for a real or simulated process during or after catalyst failure reveals the rate, extent, and nature of the degradation process. Accordingly, it is important to know how degradation processes and catalyst properties such as metal dispersion, metal concentration, and extent of reduction to the metal might affect the measurement of metal particle size.

Previous studies of metal particle size and various methods for estimating this property have been summarized and discussed in reviews by Dorling (*1*), Whyte (*2*), and Farrauto (*3*). Farrauto discussed the Group VIII metals individually, indicating what he considered to be the best methods for studying these metals. In the case of nickel, he mentioned that H_2 chemisorption was most commonly used although X-ray diffraction (XRD) and transmission electron microscopy (TEM) were also considered useful techniques. It is also clear from recent literature that magnetic susceptibility measurements can also be used to measure nickel crystallite size and size distribution (*4–6*). Farrauto pointed out, however, that a combination of at least two methods is essential for accurate determination of metal particle size for a given catalyst system and that work defining the limitations of various techniques for measuring metal particle size and metal surface area had not yet been reported in the case of supported nickel.

Indeed, a careful search of more recent literature reveals that no such definitive work has yet appeared. Moreover, except for two very recent studies (*6, 7*) the use of

0021-9517/81/010186-21$02.00/0
Copyright © 1981 by Academic Press, Inc.
All rights of reproduction in any form reserved.

two or more quantitative methods to accurately define nickel particle size has not been reported. For example, Van Hardeveld and co-workers (*8, 9*) used XRD and TEM in addition to adsorption techniques to study Ni/SiO_2; however, their TEM work was not very quantitative. Moreover, their estimates of metal particle size from XRD were in only approximate agreement with corresponding estimates from H_2 adsorption.

The present study was undertaken to (i) determine and compare the accuracy and limitations of various techniques for measuring nickel metal particle size and (ii) determine the effects of catalyst properties (i.e., metal dispersion, nickel concentration, and support), catalyst preparation, pretreatment, and sintering on the measurement of metal particle size. Three different techniques were used: H_2 chemisorption, XRD line broadening, and TEM. This paper reports and discusses results obtained for Ni/SiO_2, Ni/Al_2O_3, and Ni/TiO_2 catalysts using these techniques to measure metal particle size and using TEM to determine crystallite size distribution and morphology.

EXPERIMENTAL

Catalyst Preparation

Nickel alumina. Nickel alumina catalysts were prepared using a procedure developed previously in this laboratory (*10, 11*) involving impregnation toincipient wetness of Kaiser SAS 5 × 8-mesh alumina (300 m^2/g) which had been previously calcined for 2 h at 873 K. The impregnated samples were dried 12–16 h at 353–373 K in a forced-air-circulation oven. Three impregnations were used in order to distribute the active catalytic material more uniformly throughout the support.

Nickel silica. Two silica-supported nickel catalysts were prepared using a homogeneous, controlled-pH precipitation described by previous workers (*5, 12*). A predetermined weight of $Ni(NO_3)_2 \cdot 6H_2O$ was dissolved in deionized water, according to the percentage of nickel desired in the catalyst. Silica (Cab-O-Sil M-5, Cabot Corporation, 200 m^2/g), precalcined at 873 K for 2 h, was then added to this solution forming a slurry. The pH of the slurry was initially lowered to 2.5 using concentrated nitric acid, after which solid urea was added in the ratio of 5 parts urea to 1 part nickel by weight. The slurry was heated using a boiling water bath (369 K) with constant stirring for at least 30 h, cooled while stirring, and filtered under vacuum. The catalyst precipitate was then dried overnight at 353 K after which it was ground into a powder. Two other catalysts were prepared using the impregnation procedure described under nickel alumina. Atomic adsorption spectrometry was performed by Rocky Mountain Geochemical Corporation to determine the actual percentage loading of each catalyst (Table 1).

Nickel titania. Nickel titania catalysts were prepared by impregnation of TiO_2 (Anatase form, Degussa, Inc., 50 m^2/g) using a procedure identical to that for the nickel alumina catalysts. Several impregnations were also used to distribute the metal more evenly. All catalysts were reduced 14–16 h in flowing H_2 at 725 K according to procedures previously described (*11, 13, 14*).

Procedure

Chemisorption measurements. Chemisorptive uptakes were measured using a constant-volume glass system evacuated by mechanical and oil diffusion pumps, isolated by a liquid nitrogen trap. A Texas Instruments quartz Bourdon gauge was used in making the adsorption pressure measurements. Calibration and use of the chemisorption system were previously described (*10, 13, 14*). Typical room temperature adsorption isotherms for H_2 were determined by plotting micromoles of H_2 adsorbed vs pressure. The uptake due to chemisorption was then determined by extrapolating the straight-line portion of the isotherm to zero pressure (*10, 11*).

TABLE 1

Composition, Values of H_2 Uptake, Percentage Reduction, and Percentage Dispersion for Catalysts Studied

Catalyst and pretreatment	Ni (wt%)	H_2 uptake[a] (μmol/g)	Percentage reduction[b]	Percentage dispersion[c]
Ni/Al_2O_3[d]	15			
Fresh		188	84	17
Sintered				
in H_2 at 1023 K, 72 h		122	—	9.5
in 3% H_2O/H_2 at 1023 K, 13 h		121	—	9.5
Ni/Al_2O_3[d]	23	305	97	16
Ni/SiO_2[d]	2.7			
Fresh		85	71	51
Calcined 573 K, 3 h		35	71	16
Ni/SiO_2[e]	3.6			
Fresh		81	71	37
Ni/SiO_2[e]	13.5			
Fresh		442	93	41
Sintered in H_2				
923 K, 50 h		252	—	22
973 K, 50 h		178	—	15
1023 K, 50 h		177	—	15
Ni/SiO_2[d]	15			
Fresh		217	90	19
Calcined 773 K, 22 h		61	82	5.8
Ni/TiO_2[d]	2.8			
Fresh		20	74	11
Ni/TiO_2[d]	15			
Fresh		49	90	4.3
Sintered 3 h at 1023 K in H_2		1	90	0.1

[a] Total H_2 uptake at 298 K.

[b] Percentage reduction of nickel to the metal based on O_2 uptake at 725 K; in the case of Ni/TiO_2 measured by $Ni(CO)_4$ extraction.

[c] Calculated according to Eq. (1) with percentage reduction taken into account.

[d] Prepared by impregnation.

[e] Prepared by controlled pH precipitation.

Extents of reduction to metallic nickel were measured for Ni/Al_2O_3 and Ni/SiO_2 catalysts from oxygen uptakes at 723 K and for Ni/TiO_2 catalysts by $Ni(CO)_4$ extraction as described by Bartholomew and Farrauto (*11*).

Percentage dispersion (percentage exposed) was calculated from H_2 uptake according to the equation

$$\%D = \frac{1.17\,X}{Wf}, \qquad (1)$$

where X = H_2 uptake in micromoles per gram of catalyst, W = weight percentage of nickel, and f = fraction of nickel reduced to the metal. This was based on the assumption that unreduced nickel was present in a separate dispersed layer in intimate contact with the support (*15*). The average nickel crystallite diameter (surface-averaged) was calculated using

$$d_s = \frac{971}{\%D} \qquad (2)$$

based on the assumption of spherical crystallites of uniform size.

Electron microscopy. Sample preparation was similar to that of Basset *et al.* (*16*). Finely ground catalyst was suspended in *n*-butyl alcohol and ultrasonically dispersed for 5 min. The large particles in the suspension were permitted to settle out for 1 min and a drop of the fine suspension was placed on a fine mesh copper screen. A holey-carbon coated copper grid was then placed on the screen, coating side touching the droplet. This permitted the droplet to evaporate leaving a uniform deposit of catalyst on the carbon-coated side. After coating with an additional layer of carbon for increased stability the impregnated grid was placed in the microscope.

TEM measurements were conducted using a Hitachi HU-11E electron microscope, capable of better than 1 nm resolution. To unambiguously identify metal crystallites all electron micrographs were closely compared to electron micrographs of the support. Metal crystallites of 1.5-nm diameter or larger could be observed (calibrated using the technique of Heidenreich *et al.* (*17*)). Smaller-diameter particles were impossible to distinguish accurately from the support. All catalyst samples were examined at a magnification of 71,500X. An average of 900–1000 particles from at least ten pictures were counted for each sample using enlarged photographs at a magnification of 371,800X. Accuracy to within ±0.3 nm was obtained for the micrographs analyzed.

Particle size distributions were obtained by tabulating the number of particles in a specific size range, i.e., 1.1 to 2.0 nm. Histograms were prepared by determining the percentage of the total particles in each size range. Average particle or average crystallite[1] diameter in the form of a surface mean diameter (d_s) or a volume mean diameter (d_v) was calculated from the crystallite size distribution according to the following equations in which n_i is the number of particles having a characteristic diameter d_i (within a given diameter range):

$$d_s = \frac{\sum_i n_i d_i^3}{\sum_i n_i d_i^2}, \tag{3}$$

$$d_v = \frac{\sum_i n_i d_i^4}{\sum_i n_i d_i^3}. \tag{4}$$

X-Ray diffraction line broadening. X-Ray measurements were performed at the University of Utah using a Phillips diffractometer with CuK_α radiation and a graphite monochrometer. Analysis of the line broadening for the (111) and (200) peaks according to Klug and Alexander (*18*) and Topsoe (*19*) yielded a volume-mean diameter for comparison with TEM results.

RESULTS

Table 1 lists the pretreatment, composition, H_2 uptake, percentage reduction, and percentage dispersion (percentage exposed) for each catalyst studied. The percentage dispersion data indicate that fresh Ni/SiO_2 catalysts, especially those prepared by controlled pH precipitation, were very well dispersed. Pretreatments involving precalcination or sintering in H_2 reduced nickel dispersion by factors of 2–3. Thus by means of different pretreatments and preparations it was possible to obtain Ni/SiO_2 catalysts representing a wide range of dispersion. Fresh Ni/Al_2O_3 and Ni/TiO_2 catalysts were moderately dispersed; sintering in H_2 at 1023 K effected a 40% loss of dispersion for Ni/Al_2O_3, whereas Ni/TiO_2 completely lost its ability to adsorb H_2. However, as will be explained later, this loss of ability to adsorb H_2 does not mean that the metal surface area was completely lost.

Representative TEM micrographs for Al_2O_3, SiO_2, TiO_2 supports and Ni/Al_2O_3, Ni/SiO_2, and Ni/TiO_2 catalysts are shown

[1] According to Whyte (*2*) particle size and crystallite size can be assumed to be the same in very small crystallites.

TABLE 2

Crystallite Size Distributions for Fresh and Sintered Ni/SiO_2 and Ni/TiO_2

Catalyst	Range (nm)										
	1.1–2.0	2.1–3.0	3.1–4.0	4.1–5.0	5.1–6.0	6.1–7.0	7.1–8.0	8.1–9.0	9.1–10.0	10.1–11.0	11.1–
13.5% Ni/SiO_2											
Fresh	8[a]	80	10	1	1	0	0	0	0	0	0
Sintered[b]											
923 K	5	48	23	10	12	1	0.5	0.5	0	0	0
973 K	0.5	25	16	9	27	8	5	6	1.8	1.4	0.3
1023 K	0.8	15	11	10	30	11	11	8	1.5	1.5	0.2
15% Ni/TiO_2											
Fresh	4	7	11	30	4	9	12	3	10	2	8
Sintered[c]	0	0	0	0	0	0	0	3	1	2	94

[a] Values are expressed as percentage of particles in each size range.
[b] 50 h each in flowing H_2.
[c] 2 h at 1023 K in flowing H_2.

in Figs. 1, 3–4, and 8–10 while histograms of crystallite size distributions determined from micrographs are presented in Figs. 2 and 5–7 for Ni/Al_2O_3 and Ni/SiO_2 catalysts. Sample crystallite size distributions are also listed in Table 2 for Ni/SiO_2 and Ni/TiO_2 catalysts for which no histograms are provided. A more detailed listing of crystallite size distributions from this study is available elsewhere (*20*).

From crystallite size distributions average crystallite diameters were calculated for Ni/Al_2O_3, Ni/SiO_2 and Ni/TiO_2 catalysts according to Eqs. (3) and (4). These are compared in Tables 3–5 with crystallite diameters from H_2 chemisorption and XRD. A more detailed description of these data is provided separately for each catalyst.

Ni/Al_2O_3

Ni/Al_2O_3 samples were generally very difficult to analyze with the electron microscope because of insufficient contrast between nickel crystallites and the pore structure of the alumina support (see Fig. 1). This was particularly true of catalysts having very high (>20 wt%) or low (<10%) nickel concentrations. This lack of contrast is mainly a result of the fine pore structure of γ-Al_2O_3; indeed some of the small pores have the appearance of cylindrical or spherical particles depending upon the angle from which they are viewed (see Fig. 1a). However, close examination of micrographs of the 15% Ni/Al_2O_3 (Fig. 1b) revealed areas of sufficient contrast between the needle-shaped support particles and the spherical nickel crystallites to allow a particle size distribution and an average particle size to be determined. Even better contrast between support and metal was evident in sintered samples because the metal particles were significantly larger than in the fresh sample.

Experimental difficulties were also experienced in estimating average crystallite size for Ni/Al_2O_3 catalysts from H_2 chemisorption and XRD. In a separate detailed investigation of H_2 and CO adsorption on Ni/Al_2O_3 in this laboratory (*15*), evidence was obtained suggesting that H_2 adsorption is suppressed (i.e., $H/Ni_s < 1$) in Ni/Al_2O_3 catalysts containing less than 3 wt% Ni. Accordingly, reliable estimates of d_s could be obtained in Ni/Al_2O_3 catalysts having metal concentrations higher than 3%. From XRD scans of nickel over a range of loadings from 9 to 23% (*21*) it was found that (i) the most prominent peak for Ni(111) was completely obscured by a broad peak for γ-Al_2O_3 and (ii) the second most prominent peak, Ni(200), was absent in 9% Ni/Al_2O_3, weak in 15% Ni/Al_2O_3 and of moderate intensity in 23% Ni/Al_2O_3. Thus estimates of average crystallite diameter from XRD were marginal for 15% Ni/Al_2O_3 and satisfactory for 23% Ni/Al_2O_3.

Values of the surface mean diameter d_s obtained from H_2 chemisorption and TEM (Table 3) were generally in very good agreement for fresh and sintered samples. The largest disagreement occurred in the case of the 15% Ni/Al_2O_3, where d_s from TEM was 33% lower than that from H_2 adsorption. The X-ray pattern for fresh 15% Ni/Al_2O_3 was too weak to enable a quantitative estimate of d_v, whereas values of the volume mean diameter for sintered 15% Ni/Al_2O_3 from XRD were lower by as much as a factor of 2 compared to those from TEM. On the other hand very good agreement was evident for d_v (TEM) and d_v (XRD) in the case of 23% Ni/Al_2O_3.

From the histogram in Fig. 2 it is apparent that sintering of Ni/Al_2O_3 in H_2 causes a significant broadening of the crystallite size distribution and a shift to higher crystallite sizes (compare Figs. 2a and b). The effect is obviously greater when a small amount of H_2O is present (see Fig. 2c).

Ni/SiO_2

Determination of crystallite size in Ni/SiO_2 catalysts with TEM was facilitated by the excellent contrast between metal and nonporous support (compare Fig. 3a with 3b and c). This was true of samples of

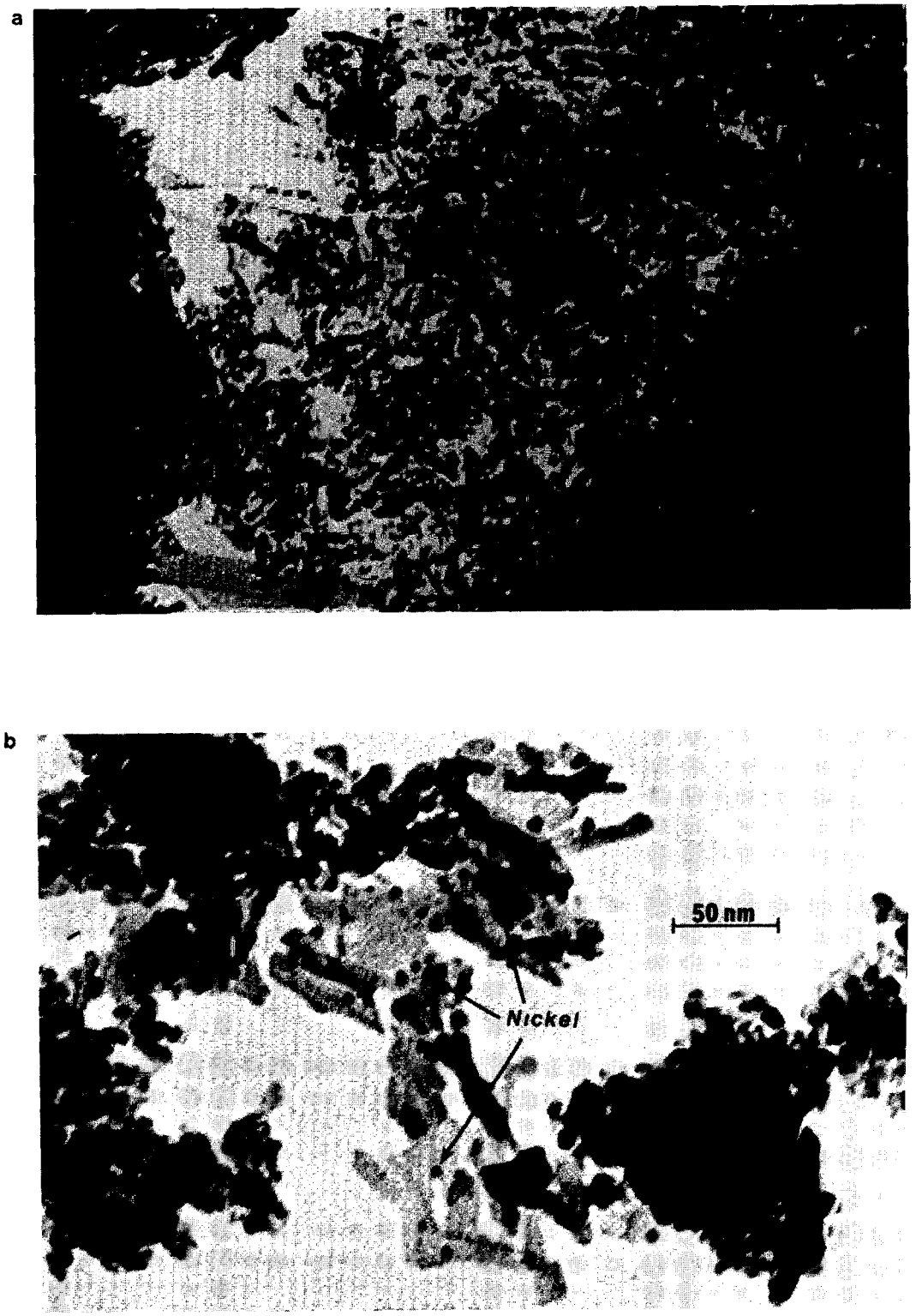

FIG. 1. Electron micrographs of (a) γ-alumina support and (b) 15% Ni/Al_2O_3.

TABLE 3

Comparison of Average Crystallite Diameters for Ni/Al_2O_3 Catalysts

Catalyst and pretreatment	d_s (nm)[a] H_2 Ads.	d_s, d_v (nm)[b] TEM	d_v (nm)[c] XRD
15% Ni/Al_2O_3			
Fresh	5.6	3.7, 4.6	<3
Sintered[d]	10	9.3, 11	4.6
Sintered in H_2O[e]	10	10, 12	4.9
23% Ni/Al_2O_3	6.1	6.0, 6.4	6.8

[a] Surface averaged values calculated from Eq. (2).
[b] Surface averaged values, volume averaged values from Eqs. (3) and (4).
[c] Volume averaged values from the Scherrer equation (*18*).
[d] 72 h at 1023 K in H_2.
[e] 13 h at 1023 K in 3% H_2O/H_2.

both low (2.7 or 3.6 wt%) and moderately high (13.5–15%) nickel loading (compare Figs. 3b and c), although the particle density was significantly less in the 3% catalysts, requiring analysis of many more micrographs to arrive at comparable counting statistics. H_2 chemisorption measurements were also found to be without complication and quite reproducible on Ni/SiO_2 over the full range of loading and dispersion. However, determination of crystallite size from XRD was generally not possible because most of the Ni/SiO_2 catalysts contained a large fraction of particles below the detection limit of XRD of about 3.0–4.0 nm. The XRD patterns for samples containing

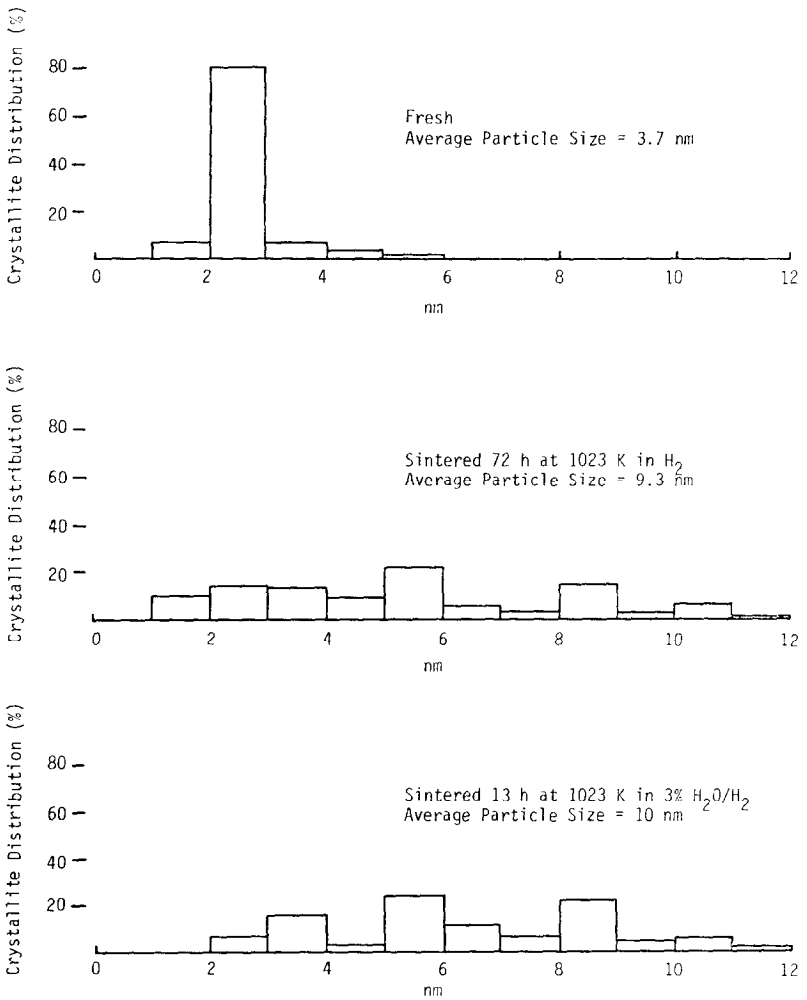

FIG. 2. Crystallite size histograms of fresh and sintered 15% Ni/Al_2O_3.

mostly medium–large crystallites were easily analyzed because of the absence of support interferences.

Crystallite size estimates from TEM and H_2 adsorption for Ni/SiO_2 catalysts (Table 4) were generally in very good agreement ($\pm 10\%$). However, good to fair (30–50%) agreement between d_s values was observed for 2.7% Ni/SiO_2 and fresh 15% Ni/SiO_2. Histograms for these two catalysts (Figs. 5 and 6) reveal the crystallite size distribution to be very narrow for fresh 2.7% Ni/SiO_2 and very broad for fresh 15% Ni/SiO_2 and calcined 2.7% Ni/SiO_2. Accordingly, the lower values of d_s from chemisorption compared to those from TEM for calcined 2.7% and fresh 15% Ni/SiO_2 are easily explained by the broad particle size distributions and

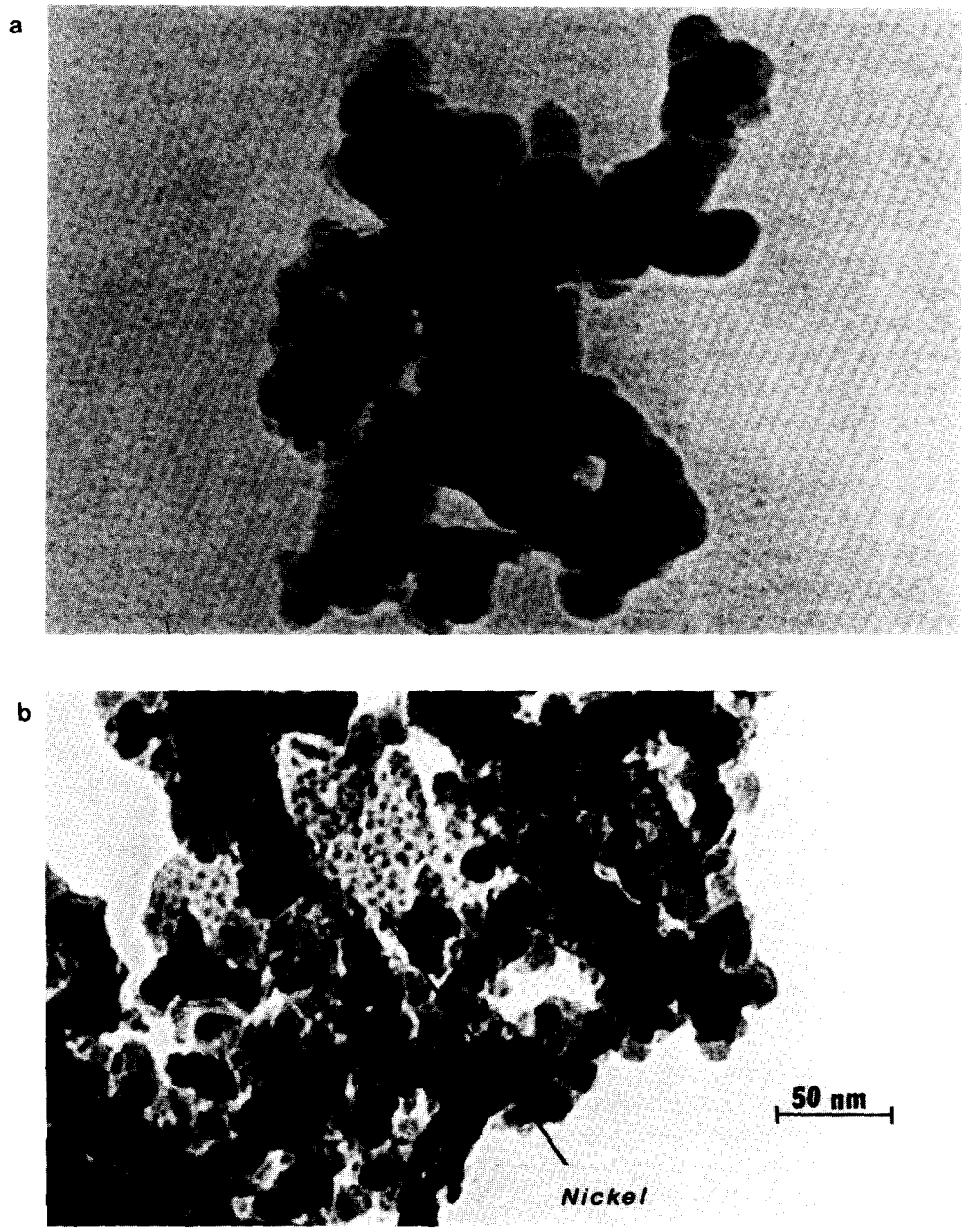

FIG. 3. Electron micrographs of (a) silica support, (b) 3.6% Ni/SiO_2, and (c) 13.5% Ni/SiO_2.

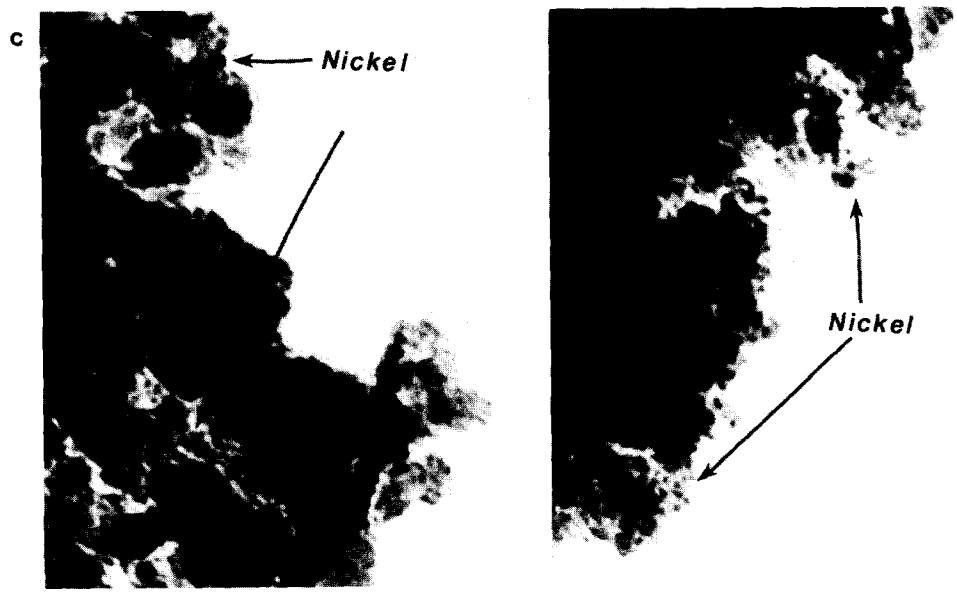

FIG. 3—*Continued*

the fact that estimation of average crystallite size from H_2 adsorption is most sensitive to the smaller crystallite sizes having larger surface to volume ratios while d_s from TEM calculated according to Eq. (3) involves d_i to the second and third powers, thus giving the greatest weight to the large particles. In the case of the precalcined 2.7% Ni/SiO_2, there is an additional effect which undoubtedly contributes to the discrepancy in d_s values, namely, the presence of thin, electron-transparent particles (Fig. 4).

TABLE 4

Comparison of Average Crystallite Diameters for Ni/SiO_2 Catalysts

Catalyst and pretreatment	d_s (nm)[a] H_2 Ads.	d_s, d_v (nm)[b] TEM	d_v (nm)[c] XRD
2.7% Ni/SiO_2			
Fresh	1.9	2.9	—
Calcined 3 h at 573 K	5.6	11	—
3.6% Ni/SiO_2			
Fresh	2.6	2.7, —	—
13.5% Ni/SiO_2			
Fresh	2.4	2.9, —	<3
Sintered in H_2			
923 K, 50 h	4.4	4.1, 4.5	2.8
973 K, 50 h	6.3	6.3, 7.1	5.4
1023 K, 50 h	6.3	6.9, 8.0	4.8
15% Ni/SiO_2			
Fresh	5.1	8.1, 9.4	12
Calcined 22 h at 773 K	17	19, 24	19

[a] Surface averaged values calculated from Eq. (2).
[b] Surface averaged values, volume averaged values from Eqs. (3) and (4).
[c] Volume averaged values from Scherrer equation (*18*).

Estimates of d_v from XRD (for those cases where it was possible to obtain data) were typically 30–40% smaller than corresponding d_v values from TEM in relatively well-dispersed Ni/SiO_2 (e.g., 13.5% Ni/SiO_2) and in good agreement for the moderately or poorly dispersed samples of 15% Ni/SiO_2 (see Table 4).

The histograms in Fig. 7 show that sintering of Ni/SiO_2 at progressively higher temperatures in H_2 results in a progressively broader crystallite size distribution and a shift to larger crystallite diameters. The histogram obtained for treatment of Ni/SiO_2 at 1023 K for 50 h in H_2 (Fig. 7) is very similar to that obtained for Ni/Al_2O_3 after treatment at 1023 K for 72 h in H_2 (see Fig. 2).

Ni/TiO_2

Figure 8a shows a micrograph of the TiO_2

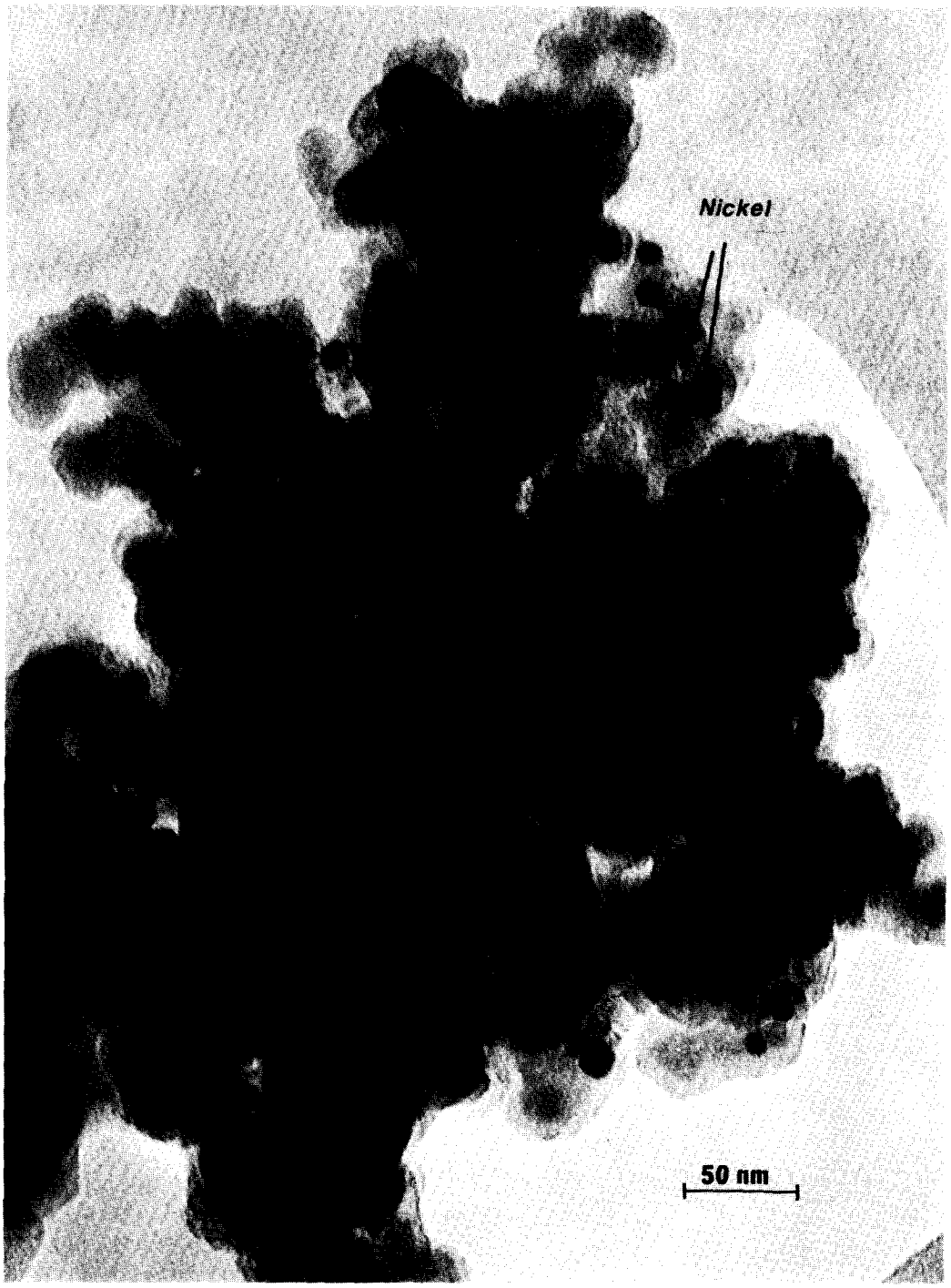

FIG. 4. Electron micrograph of calcined 2.7% Ni/SiO_2.

support. Its structure is characterized by nonporous particles, ranging in size from less than 10 to 100 nm but primarily in the range of 15–40 nm. Micrographs of Ni/TiO_2 (Figs. 8b, c, 9, 10) reveal the presence of thin, electron-transparent crystallites on

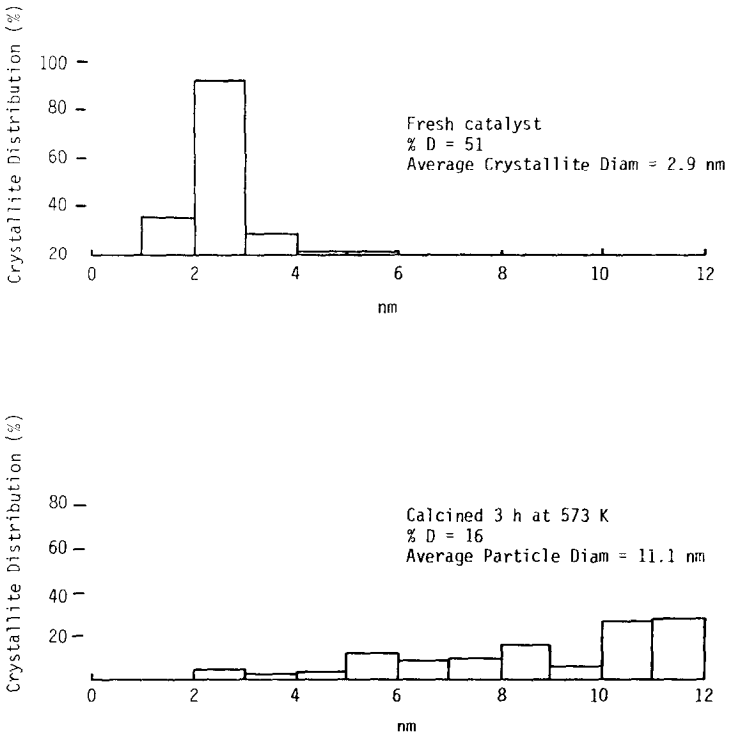

FIG. 5. Crystallite size histograms of fresh and calcined 2.7% Ni/SiO_2.

the support, as well as a few dense particles which may be either nickel or support particles or both.

In contrast to Ni/Al_2O_3 and Ni/SiO_2, crystallite diameters from H_2 adsorption and TEM for Ni/TiO_2 were in relatively poor agreement. For example, values of d_s from H_2 adsorption for fresh 2.8 and 15% Ni/TiO_2 exceeded those from TEM by almost a factor of 2; after sintering the 15% Ni/TiO_2 3 h at 1023 K, the d_s value estimated from H_2 adsorption was a factor of 30 greater than d_s from TEM. In addition to a few "raft-like" crystallites the micrograph of the 15% Ni/TiO_2 sintered at 1023 K (Fig. 10) revealed a "cloudy" surface phase which had not been previously observed in other samples tested. There was no evidence in the X-ray pattern for the sintered sample of nickel oxides or nickel spinel phases. Only the pattern for Ni metal was observed. The data in Table 5 indicate good

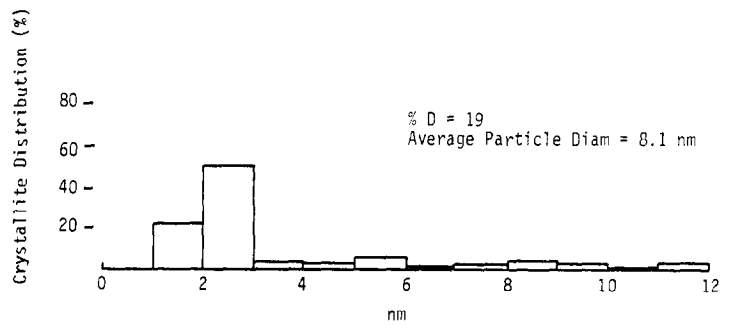

FIG. 6. Crystallite size histogram of fresh 15% Ni/SiO_2.

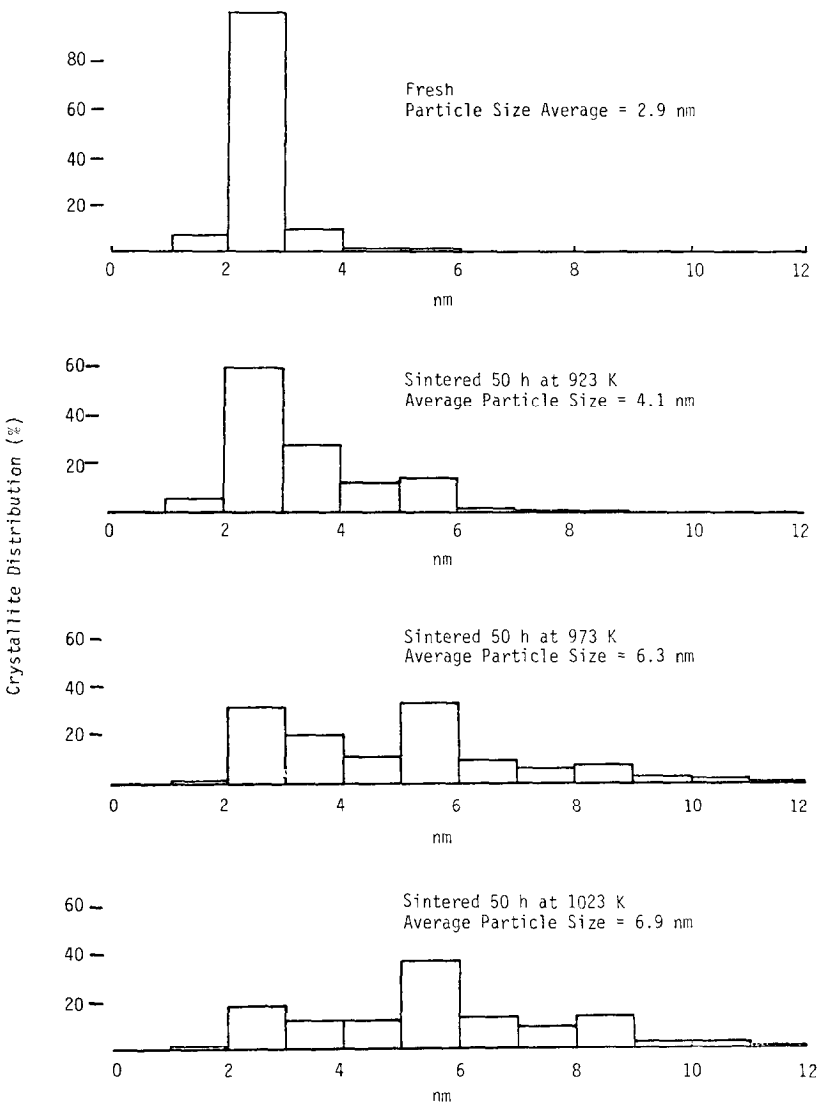

FIG. 7. Crystallite size histograms of fresh and sintered 13.5% Ni/SiO_2.

agreement between d_v values from TEM and XRD for fresh and sintered 15% Ni/TiO_2 samples.

DISCUSSION

To our knowledge, this investigation is the first quantitative TEM study of Ni/Al_2O_3, Ni/SiO_2, and Ni/TiO_2 catalysts. This study also includes the first quantitative comparison of average nickel crystallite size from TEM, H_2 adsorption, and XRD, although similar previous studies were reported for supported Pt (*22*) and Pd (*23*).

In previous studies of Ni/SiO_2 (*8, 9*) and Ni/Al_2O_3 (*24*) catalysts, comparisons were made of average crystallite size from H_2 chemisorption and XRD, the results showing, as in this study, only fair agreement (within 30–50%). The estimates of Brooks and Christopher (*24*) of nickel surface area from H_2 chemisorption and XRD varied by as much as 200–300%; moreover, their estimates of surface area from XRD for a given

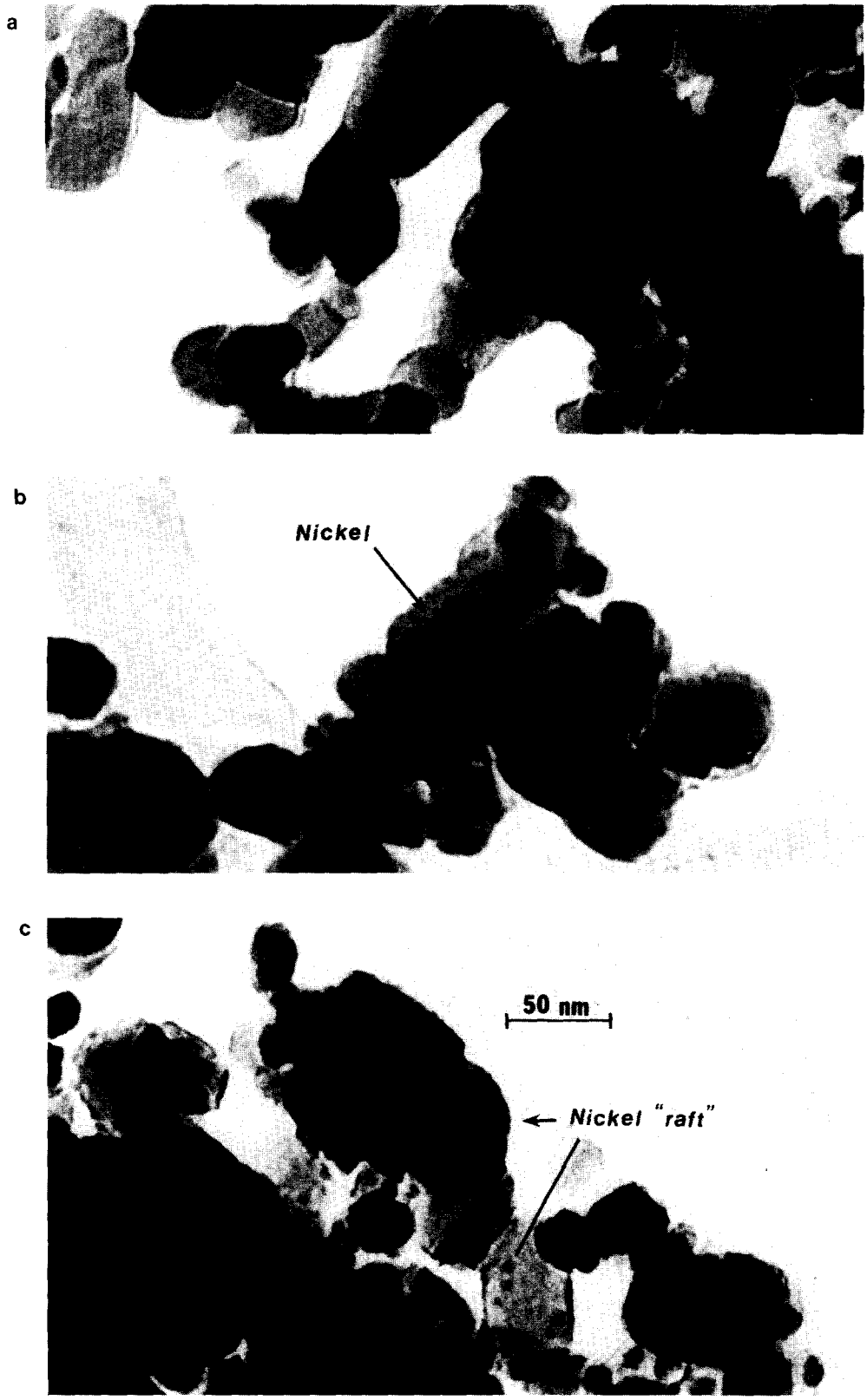

FIG. 8. Electron Micrographs of (a) titania support; and (b, c) 2.8% Ni/TiO_2.

FIG. 9. Electron micrograph of 15% Ni/TiO_2.

sample varied by as much as 200–300%. Van Hardeveld and Hartog (9) characterized their Ni/SiO_2 catalysts by means of TEM but reported only qualitative information indicating either broad or sharp particle size distributions.

Accuracy and Range of Application for TEM, H_2 Adsorption, and XRD in Determining Nickel Crystallite Size

On the basis of the results obtained in this investigation, estimated accuracies and

FIG. 10. Electron micrograph of sintered 15% Ni/TiO_2.

ranges of application for TEM, H_2 adsorption and XRD are summarized in Tables 6 and 7.

Table 6 suggests that H_2 adsorption and TEM are both very accurate techniques for estimating nickel crystallite size in Ni/SiO_2 catalysts. Table 7 indicates this to be true over a wide range of nickel loadings and dispersions. H_2 adsorption is likewise very accurate and widely applicable to determi-

TABLE 5

Comparison of Average Crystallite Diameters for Ni/TiO_2 Catalysts

Catalyst and pretreatment	d_s (nm)[a] H_2 Ads.	d_s, d_v (nm)[b] TEM	d_v (nm)[c] XRD
2.8% Ni/TiO_2			
Fresh	8.7	5.5, —	—
15% Ni/TiO_2			
Fresh	23	9.9, 11.5	15, 10
Sintered[d]	1060	32, 35	26, 21

[a] Surface averaged values calculated from Eq. (2).

[b] Surface averaged and volume averaged values from Eqs. (3) and (4).

[c] Volume averaged values for the (111) and (220) crystal planes, respectively, calculated from the Scherrer equation (*18*).

[d] 3 h at 1023 K in H_2.

nation of crystallite size in Ni/Al_2O_3 catalysts (Tables 6 and 7). Indeed, these conclusions are supported by two observations in this study: (i) agreement of d_s values from H_2 adsorption and TEM within ±10% (Tables 3 and 4) and (ii) reproducibility of each of these techniques in measuring average crystallite size to within about ±10%. Adams *et al.* (*22*) also reported errors in their TEM measurements of about 10%. In a recently ASTM-conducted round robin (*25*), the standard deviations for H_2 adsorption measurements on 12% Ni/Al_2O_3 from sample to sample (23 different samples) and from laboratory to laboratory (8 different labs) were 7.5 and 6.7% of the mean, respectively.

The accuracy of crystallite size measurements in Ni/Al_2O_3 catalysts by TEM is only

TABLE 6

Accuracy of Crystallite Size Measurements

Catalyst	H_2 Ads.	TEM	XRD
Ni/SiO_2	Very good (±10%)	Very good	Fair (±30–50%)
Ni/Al_2O_3	Very good	Fair–good	Fair
Ni/TiO_2	Poor (high by 50–100%)	Good (±20%)	Fair–good

TABLE 7

Range of Nickel Concentration and Metal Dispersion in Crystallite Size Measurements

Catalyst	H_2 Ads.	TEM	XRD
Ni/SiO_2	Full	Full	wt% > 10 d_v > 3 nm
Ni/Al_2O_3	wt% > 3	10–25 wt% $d_{pore} > d_s$	wt% > 20 d_v > 3 nm
Ni/TiO_2	wt% > 30–50%? low T_{redn}	Full wt% $d_s < d_{support}$	wt% > 10 d_v > 3 nm

fair to good and the range of loadings and dispersions limited because of the relatively poor contrast between metal crystallites and support as a consequence of the porous support structure (see Fig. 1). This fact probably explains why most of the previous TEM studies were conducted using silica or carbon supports rather than Al_2O_3 (*2*).

H_2 adsorption is apparently a poor technique for estimating crystallite size in Ni/TiO_2 since it results in abnormally high estimates compared to TEM and XRD (see Table 5). This can be attributed to suppression of H_2 adsorption as a result of strong electronic interactions between nickel crystallites and the TiO_2 support (*7, 27*), or the formation of a surface $NiTiO_x$ ($x < 2$) intermetallic as hypothesized for noble metal/TiO_2 systems (*26*). The factor of 2 larger crystallite diameter from H_2 adsorption for fresh Ni/TiO_2 catalysts might also be explained by inaccuracies (estimated at 50–75%) resulting from the assumption of spherical particles when they are actually more like flat plates. The accuracy of crystallite size measurements in Ni/TiO_2 catalysts by TEM was better than for Ni/Al_2O_3, although approximately 20–30% of the particles in Ni/TiO_2 could be assigned to either support or metal; hence the accuracy is designated as "good."

Assuming that H_2 adsorption and TEM can be used as standards for Ni/SiO_2 and Ni/Al_2O_3, the accuracy of estimates of average crystallite size from XRD (see Tables 3 and 4) are only fair (±30–50%). This conclusion finds support from Whyte (*2*) who assessed the absolute accuracy of X-ray

TABLE 8

Advantages and Disadvantages of Experimental Techniques for Measuring Nickel Crystallite Size

Method	Advantages	Disadvantages
H_2 Adsorption	Convenient, inexpensive Fast Accurate Measures particles of all sizes	Affected by contamination and metal–support interactions Adsorption stoichiometry may be variable with dispersion or metal loading
TEM	Accurate Direct measurement of size More information, e.g., size distribution, particle shape, texture	Expensive Tedious Lack of contrast between crystallites and support Doesn't see very small particles (<1.5 nm)
XRD	Convenient	Expensive Inaccurate Support interferences Insensitive to low metal loadings and small particles (<3 nm)

line broadening estimates to be no better than 25–50% for metal particles larger than 3.5 nm. XRD has also rather severe limitations in terms of metal dispersion and metal concentration (see Table 7). Indeed, the data from this study show that X-ray diffraction peaks were not observable in nickel catalysts in which d_s or d_v was less than 3–4 nm and metal loadings were less than 10% (see Tables 3–5). Because of support interferences in Ni/Al_2O_3 which obscure the most prominent nickel peak (Ni(111)), nickel loadings of greater than 20% are necessary to enable observation of well-defined secondary peaks such as Ni(200). However, because metal crystallites were generally larger in Ni/TiO_2 catalysts (than in Ni/SiO_2 or Ni/Al_2O_3), agreement between d_v (TEM) and d_v (XRD) was better and usually within 20–40% (see Table 5).

Based on the experience gained in this investigation advantages and disadvantages of the three different techniques used to estimate crystallite size are summarized in Table 8. Our experience leads us to the conclusion that H_2 adsorption is the most accurate, convenient and inexpensive technique for measuring average crystallite size of Ni/Al_2O_3 and Ni/SiO_2 catalysts. Although the extent and stoichiometry of adsorption may be affected by surface contaminants (e.g., oxygen or sulfur) and/or metal–support interactions, the former problems can be avoided by careful adherence to accepted chemisorptive vacuum techniques. Effects of metal–support interactions are not a problem in Ni/SiO_2 or moderately dispersed Ni/Al_2O_3 (*27*). Indeed, the very good agreement for estimates of d_s from H_2 adsorption and TEM is strong evidence that room temperature hydrogen chemisorption occurs with a stoichiometry of one hydrogen atom per surface nickel atom in Ni/SiO_2 and Ni/Al_2O_3 catalysts. Implications of this well-behaved adsorption of H_2 on nickel have been discussed in a separate paper dealing with the stoichiometry of H_2 and CO on supported nickel (*15*).

TEM has the distinct advantage of providing the most direct measurement of crystallite size. In addition to being very accurate it provides information not available from the other techniques such as size distribution, particle shape, and texture. Unfortunately it is a comparatively expen-

sive, time-consuming method for measuring average crystallite size because of the large number of particles (and micrographs) that must be counted for accurate analysis.

Compared to H_2 adsorption and TEM, XRD is a relatively unreliable, inaccurate method of estimating average crystallite diameter. Diffraction patterns for the metal are sometimes obscured by broad intense peaks of highly porous supports such as γ-Al_2O_3. Except in those systems where H_2 adsorption is not reliable (e.g., Ni/TiO_2) it is not recommended as a quantitative technique for measurement of nickel crystallite size.

Characterization by TEM of Crystallite Size Distribution and Crystallite Morphology and Its Application to Supported Nickel

In addition to estimates of average crystallite size, TEM provides useful information not provided by other techniques, such as crystallite size distribution, crystallite shape and the extent of interaction of crystallites with the support. Examples of how these properties provide insight into preparation, reaction, and degradation processes as well as the morphology of the catalyst surface are provided by the data from this study and are discussed below.

Effects of catalyst preparation on crystallite size distribution. The data of this study (Tables 1 and 4 and Figs. 6 and 7) establish that compared to preparation by impregnation, the controlled-pH precipitation produces Ni/SiO_2 catalysts with much narrower crystallite size distributions and smaller average crystallite sizes in agreement with earlier workers (*5, 12*). The size distribution data for fresh 2.7 and 13.5% Ni/SiO_2 (Figs. 5 and 7) are very similar to those obtained by Richardson and Dubus (*5*) from magnetic measurements; moreover, the average crystallite diameter measured by TEM for our 13.5% Ni/SiO_2 of 2.9 nm is in excellent agreement with their value of 3.0 nm for a precipitated 17% Ni/SiO_2 reduced 15 h at 673 K. The excellent agreement of the particle size measurements from the two studies is quite gratifying, considering that the catalysts were prepared in two separate laboratories and that the crystallite size measurements were conducted using two different techniques. We conclude, therefore, that TEM and magnetic methods are capable of providing measurements of crystallite size and size distribution with the same degree of accuracy.

Effects of precalcination on crystallite distribution and crystallite morphology. From Fig. 5 and Table 4 it is apparent that high-temperature calcination prior to reduction results in a significantly broader crystallite size distribution and larger average crystallite size compared to the corresponding catalyst prepared via direct reduction in H_2. This observation is entirely consistent with the results of Bartholomew and Farrauto (*11*) showing that precalcination of Ni/Al_2O_3 catalysts resulted in substantially lower nickel surface area in comparison to catalysts prepared by direct reduction.

In addition to changes in crystallite size and size distribution, calcination also effects modifications in the morphology of metal crystallites easily detectable by TEM (compare Figs. 3b and 4). For example, large, electron-translucent crystallites are evident in the micrograph for precalcined 2.7% Ni/SiO_2 (Fig. 4). In contrast, small, dense particles are evident in micrographs for Ni/SiO_2 catalysts prepared without calcination (see Figs. 3b and c). The thin, flat nature of the crystallites in Fig. 4 suggests a very intimate contact of metal and support in the precalcined catalyst.

Evidence of metal–support interactions. The micrographs in Figs. 4 and 8–10 showing the presence of thin, electron-transparent metal crystallites are, to our knowledge, the first reported for Ni/SiO_2 and Ni/TiO_2. Previous studies of Ru/SiO_2 (*28*), Rh/Al_2O_3 (*29*) and Pt/TiO_2 (*30, 31*) have provided evidence for "raft-like" metal structures which are attributed to strong

metal–support interactions. The similar, platelike structures observed in this study for Ni/TiO_2 (and calcined Ni/SiO_2) are strongly suggestive of an intimate interaction of the metal and support. Moreover, it appears that this interaction is enhanced by heating at high temperatures in H_2, as evidenced by the appearance of a new metallic phase on the surface of the support in Fig. 10. We believe this could be evidence of a surface intermetallic, $Ni–TiO_x$ ($x < 2$), formed by the high-temperature reduction. Further evidence of strong metal–support interactions in Ni/TiO_2 was provided by two recent investigations (*7*, *27*) in which significant alterations in H_2 and CO adsorption behavior and methanation activity/selectivity properties were observed.

Effects of sintering on crystallite size distribution. Sintering of Ni/Al_2O_3 and Ni/SiO_2 catalysts causes a broadening of the crystallite size distribution and a shift to a larger average crystallite size (see Figs. 2 and 7). These changes in CSD with increasing time and temperature provide useful insights into the mechanism of sintering, a topic discussed in a separate paper (*32*).

CONCLUSIONS

1. H_2 adsorption is the most convenient, accurate, and generally applicable technique for estimating average crystallite size of supported nickel.

2. TEM is a tedious but accurate technique for measuring average crystallite size *and size distribution* of nickel on supports consisting of nonporous particles, e.g., Cab-O-Sil, or containing mainly large pores. Its application to $Ni/\gamma\text{-}Al_2O_3$ is limited.

3. XRD is neither accurate nor widely applicable to estimation of particle size in supported nickel. Besides its general insensitivity to small metal particles, its application to Ni/Al_2O_3 is limited because the diffraction peaks for $\gamma\text{-}Al_2O_3$ interfere with those for nickel metal.

4. TEM and H_2 adsorption data suggest $H/Ni_s = 1$ on 3–15% Ni/SiO_2 and 15–25% Ni/Al_2O_3.

5. TEM and H_2 adsorption constitute a powerful combination for investigating metal–support interactions and sintering in supported nickel.

ACKNOWLEDGMENTS

The authors gratefully acknowledge support from the Department of Energy (DOE Contract EF-77-S-01-2729) and technical assistance by Dr. Charles H. Pitt of the University of Utah in obtaining X-ray data, Dr. Wilford M. Hess of Brigham Young University in obtaining TEM data, Dr. Richard B. Pannell, Mr. Jay L. Butler, Mr. Wayne L. Sorenson, and others of the BYU Catalysis Laboratory.

REFERENCES

1. Dorling, T. A., Warren Springs Lab., LR145(CA) (1971).
2. Whyte, T. E., Jr., *Catal. Rev.* **8**, 117 (1973).
3. Farrauto, R. J., *AIChE Symp. Ser.* **70**, 143 (1974).
4. Selwood, P. W., "Chemisorption and Magnetism." Academic Press, New York, 1975.
5. Richardson, J. T., and Dubus, R. J., *J. Catal.* **54**, 207 (1978).
6. Primet, M., Dalmon, J. A., and Martin, G. A., *J. Catal.* **46**, 25 (1977).
7. Vannice, M. A., and Garten, R. L., *J. Catal.* **56**, 236 (1979).
8. Van Hardeveld, R., and Van Montfoort, A., *Surface Sci.* **4**, 396 (1966).
9. Van Hardeveld, R., and Hartog, F., *Advan. Catal.* **22**, 75 (1972).
10. Bartholomew, C. H., Quarterly progress report submitted to ERDA, FE-1790-1, Aug. 6, 1975.
11. Bartholomew, C. H., and Farrauto, R. J., *J. Catal.* **45**, 41 (1976).
12. Van Dillen, J. A., Geus, J. W., Hermans, L. A. M., and Van der Meivben, J., *in* "Proceedings, 6th International Congress on Catalysis, (London 1976)." Chemical Society, London.
13. Pannell, R. B., Ph.D. dissertation, Brigham Young University, April 1978.
14. Bartholomew, C. H., Final report to ERDA, FE-1790-9, Sept. 6, 1977.
15. Bartholomew, C. H., and Pannell, R. B., *J. Catal.*, **65**, 390.
16. Basset, J. M., Dalmai-Imelik, G., Primet, M., and Mutin, R., *J. Catal.* **37**, 22 (1975).
17. Heidenrich, R. D., Hess, W. M., and Ban, L. L., *J. Appl. Crystallogr.* **1**, 1 (1968).
18. Klug, H. P., and Alexander, L. E., "X-ray Diffraction Procedures." Wiley, New York, 1974.

19. Topsoe, H., Ph.D. dissertation, Stanford University, November 1972.
20. Mustard, D. G., M.S. thesis, Brigham Young University, Aug. 1980.
21. Stowell, D. E., M.S. thesis, Brigham Young University, December 1976.
22. Adams, C. R., Benesi, H. A., Curtis, R. M., and Meisenheimer, R. G., *J. Catal.* **1**, 336 (1962).
23. Scholten, J. J. F., and Van Montfoort, A., *J. Catal.* **1**, 85 (1962).
24. Brooks, C. S., and Christopher, G. L. M., *J. Catal.* **10**, 211 (1968).
25. Bartholomew, C. H., Progress summary prepared for ASTM Committee D-32, November 9, 1976.
26. Tauster, S. J., Fung, S. C., and Garten, R. L., *J. Amer. Chem. Soc.* **100**, 170 (1978).
27. Bartholomew, C. H., Pannell, R. B., and Butler, J. L., *J. Catal.*, **65**, 335 (1980).
28. Prestridge, E. B., Via, G. H., and Sinfelt, H. J., *J. Catal.* **50**, 115 (1977).
29. Yates, D. J. C., Murrell, L. L., and Prestridge, E. B., *J. Catal.* **57**, 41 (1979).
30. Baker, R. T. K., Prestridge, E. B., and Garten, R. L., *J. Catal.* **56**, 390 (1979).
31. Baker, R. T. K., Prestridge, E. B., and Garten, R. L., *J. Catal.* **59**, 293 (1979).
32. Sorenson, W., and Bartholomew, C. H., in preparation, 1980.